Article

Rapid Vapor-Phase Fabrication of Organic–Inorganic Hybrid Superlattices with Monolayer Precision

Byoung H. Lee, Min Ki Ryu, Sung-Yool Choi, Kwang-H. Lee, Seongil Im, and Myung M. Sung

J. Am. Chem. Soc., **2007**, 129 (51), 16034-16041 • DOI: 10.1021/ja075664o

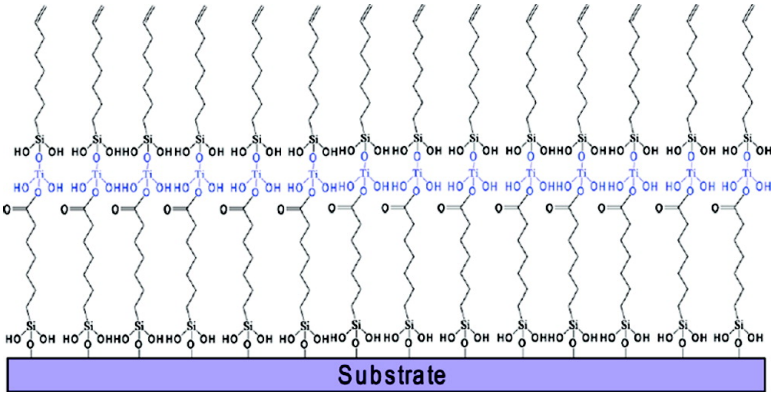

More About This Article

Additional resources and features associated with this article are available within the HTML version:

- Supporting Information
- Links to the 2 articles that cite this article, as of the time of this article download
- Access to high resolution figures
- Links to articles and content related to this article
- Copyright permission to reproduce figures and/or text from this article

View the Full Text HTML

J|A|C|S
ARTICLES
Published on Web 11/30/2007

Rapid Vapor-Phase Fabrication of Organic−Inorganic Hybrid Superlattices with Monolayer Precision

Byoung H. Lee,[†] Min Ki Ryu,[‡] Sung-Yool Choi,[‡] Kwang-H. Lee,[§] Seongil Im,[§] and Myung M. Sung*,[†]

Contribution from the Department of Chemistry, Hanyang University, Seoul 133-791, Korea, Nanoelectronic Devices Team, ETRI, Daejeon 305-700, Korea, and Institute of Physics and Applied Physics, Yonsei University, Seoul 120-749, Korea

Received July 29, 2007; E-mail: smm@hanyang.ac.kr

Abstract: We report a new layer-by-layer growth method of self-assembled organic multilayer thin films based on gas-phase reactions. In the present molecular layer deposition (MLD) process, alkylsiloxane self-assembled multilayers (SAMs) were grown under vacuum by repeated sequential adsorptions of C═C-terminated alkylsilane and titanium hydroxide. The MLD method is a self- limiting layer-by-layer growth process, and is perfectly compatible with the atomic layer deposition (ALD) method. The SAMs films prepared exhibited good thermal and mechanical stability, and various unique electrical properties. The MLD method, combined with ALD, was applied to the preparation of organic−inorganic hybrid nanolaminate films in the ALD chamber. The organic−inorganic hybrid superlattices were then used as active mediums for two-terminal electrical bistable devices. The advantages of the MLD method with ALD include accurate control of film thickness, large-scale uniformity, highly conformal layering, sharp interfaces, and a vast library of possible materials. The MLD method with ALD is an ideal fabrication technique for various organic−inorganic hybrid superlattices.

I. Introduction

Organic−inorganic hybrid thin films are drawing substantial attention because of the potential of combining the distinct properties of organic and inorganic components. The hybrid materials provide both the stable and elegant optical, electrical, and magnetic properties of inorganic components and the structural flexibility of organic components. The organic−inorganic hybrid superlattices are particularly attractive because they can provide means for combining the optimal properties of heterogeneous material systems. Furthermore, such hybrid superlattices exhibit unique optical and electrical properties which differ from their constituents.[1−3] Therefore, they provide the opportunity for developing new materials with synergic behavior, leading to improved performance or new useful properties. A key to utilizing layered organic−inorganic hybrid superlattices in advanced applications is the ability to prepare a high quality multilayer in the simplest and most reliable manner. The ability to assemble hybrid films one monolayer at a time allows for layer-by-layer control of thickness, composition, and physical properties. Such monolayer control provides an important path for the creation of new hybrid materials for organic−inorganic electronic devices and molecular electronics.

Several solution-based approaches are currently available for controlling growth with monolayer precision, such as Langmuir−Blodgett (LB)[4] and the self-assembly technique.[5] The self-assembly technique is particularly attractive because of its simplicity and potential contribution to science and technology. The formation of molecular monolayers and multilayers by self-assembly of surfactant molecules at a surface is a representative example of the self-assembly technique.[6−10] Self-assembled monolayers and multilayers are ordered organic thin films which form spontaneously on solid surfaces. Although such self-assembly techniques from solution-based methods have been extensively studied, critical issues remain to be solved such as slow formation speed, high defect density, and difficulty producing multicomponent multilayer films.[9,10] Factors contributing to organic−inorganic multilayer quality include interfacial roughness, interdiffusion between layers, layer-to-layer consistency, and layer conformality.

The preparation of high quality organic−inorganic multilayers requires a preparation method by which the above factors can be precisely controlled. Atomic layer deposition (ALD) is a potentially powerful method for preparing high quality multicomponent superlattices under vacuum conditions.[11−14] Atomic

[†] Hanyang University.
[‡] ETRI.
[§] Yonsei University.

(1) Mitzi, D. B. *Chem. Mater.* **2001**, *13*, 3283.
(2) DiSalvo, F. J. *Advancing Materials Research*; National Academy Press: Washington, DC, 1987.
(3) Costescu, R. M.; Cahill, D. G.; Fabreguette, F. H.; Sechrist, Z. A.; George, S. M. *Science* **2004**, *303*, 989.
(4) Petty, M. C. *Langmuir-Blodgett Films-An Introduction*; Cambridge University Press: Cambridge, U.K., 1996.
(5) Ulman, A. *An Introduction to Ultrathin Organic Films From Langmuir-Blodgett to Self-Assembly;* Academic Press: Boston, MA, 1991.
(6) Sagiv, J. *J. Am. Chem. Soc.* **1980**, *102*, 92.
(7) Nuzzo, R. G.; Allara, D. L. *J. Am. Chem. Soc.* **1983**, *105*, 4481.
(8) Netzer, L.; Sagiv, J. *J. Am. Chem. Soc.* **1983**, *105*, 674.
(9) Lee, H.; Kepley, L. J.; Hong, H.-G.; Mallouk, T. E. *J. Am. Chem. Soc.* **1988**, *110*, 618.
(10) Tillman, N.; Ulman, A.; Penner, T. L. *Langmuir* **1989**, *5*, 101.

10.1021/ja075664o CCC: $37.00

layer deposition (ALD) is a gas-phase thin film deposition method by using self-terminating surface reactions. During the past decade, ALD has attracted considerable attention as a method to manufacture high quality thin films and produce tailored molecular structures.[15−21] The ALD method relies on sequential saturated surface reactions which result in the formation of a monolayer in each sequence. In addition to the preparation of high quality thin films, ALD has been used to create multicomponent multilayer superlattices. Gas-phase methods, however, have not been developed to fabricate high quality organic thin films with monolayer precision nor combined with ALD for preparing organic−inorganic hybrid superlattices.

Herein, we developed a new vapor-phase deposition method of high quality self-assembled organic multilayers, called molecular layer deposition (MLD).[22,23] MLD is a gas-phase process analogous to ALD and also relies on sequential saturated surface reactions which result in the formation of a self-assembled monolayer in each sequence. In the MLD method, the high quality organic thin films can be quickly formed with monolayer precision under ALD conditions (temperature, pressure, etc). The MLD method can be combined with ALD to take advantages of the possibility of obtaining organic−inorganic hybrid thin films. The advantages of the MLD technique combined with ALD include accurate control of film thickness, large-scale uniformity, excellent conformality, good reproducibility, multilayer processing capability, sharp interfaces, and excellent film qualities at relatively low temperatures. Additionally, a vast library of materials is accessible by ALD methods, ranging from single elements to compound semiconductors to oxides, nitrides, and sulfides. Therefore, the MLD method with ALD is an ideal fabrication technique for various organic−inorganic hybrid superlattices.

II. Experimental Section

Preparation of Substrates. The Si substrates used in this research were cut from n-type (100) wafers (LG Siltron) with a resistivity in the range of 1−5 Ωcm. The Si substrates were initially treated by a chemical cleaning process proposed by Ishizaka and Shiraki which involved degreasing, HNO_3 boiling, NH_4OH boiling (alkali treatment), HCl boiling (acid treatment), rinsing in deionized water, and blow-drying with nitrogen to remove contaminants and grow a thin protective oxide layer on the surface.[24]

Atomic Layer Deposition. The oxidized Si (100) substrates were introduced into the atomic layer deposition (ALD) system Cyclic 4000 (Genitech, Taejon, Korea). The TiO_2 thin films were deposited onto the substrates using [$Ti(OCH(CH_3)_2)_4$] (Aldrich; 99.999%) and H_2O as ALD precursors.[25] Ar served as both a carrier and a purging gas. The titanium isopropoxide (TIP) and water were evaporated at 60 and 20 °C, respectively. The cycle consisted of 2 s exposure to TIP, 5 s Ar purge, 2 s exposure to water, and 5 s Ar purge. The total flow rate of the Ar was 50 sccm. The TiO_2 thin films were grown at temperatures of 150−200 °C under a pressure of 300 mtorr.

Molecular Layer Deposition. Alkene-terminated self-assembled monolayers were formed by exposing the TiO_2-coated Si substrates to [CH_2═$CH(CH_2)_6SiCl_3$] (Aldrich; 96%) with H_2O vapor at temperatures of 150−200 °C in the ALD chamber. The 7-octenyltrichlorosilane (7-OTS) and water were evaporated at 100 and 20 °C, respectively. Exposure times in this process were 5 s for 7-OTS with water vapor and 10 s for Ar purge. The total flow rate of the Ar was 50 sccm. The terminal C═C groups of the SAM were converted to carboxylic groups with ozone treatment in the ALD chamber.[26,27] The ozone was generated by an ozone-generator and dosed to the 7-OTS coated samples for 30 s at temperatures of 150−200 °C. The C═C groups of the SAM reacted with ozone to convert to carboxylic acid groups. Highly active titanium hydroxyl groups were formed on the COOH-terminated SAM by using TIP adsorption followed by exchange reaction of water molecule in order to provide highly active adsorption sites for the anchoring of the next monolayer. The molecular layer deposition of the alkylsiloxane SAMs consisted of a repetition of three steps: adsorption of 7-OTS, modification of 7-OTS with a carboxylic group using ozone, and activation of carboxylated 7-OTS with a titanium hydroxyl group.

Sample Characterization. The samples were analyzed by a JEOL-2100F transmission electron microscopy. Specimens for cross-sectional TEM studies were prepared by mechanical grinding and polishing (∼10 μm thick) followed by Ar-ion milling using a Gatan precision ion polishing system (PIPSTM, model 691). Atomic force microscopy images of the samples were obtained on a PSIA XE-100 operating in tapping mode. All XP spectra were recorded on a VG Scientific ESCALAB MK II spectrometer using Al Kα source run at 15 kV and 10 mA. The binding energy scale was calibrated to 284.6 eV for the main C(1s) peak. Each sample was analyzed at a 90° angle relative to the electron analyzer. Contact angle analysis was performed using a model A-100 Ramé-Hart NRL goniometer to measure water contact angles in room air using the Sessile drop method. The leakage current was measured using a Keithley 2400 semiconductor parameter analyzer and the capacitance was measured using a HP 4283 LCR meter at frequencies varying from 100 Hz to 1 MHz. Current−voltage curves of the pentacene-TFT were measured with a semiconductor parameter analyzer (HP4155C, Agilent Technologies). Current−voltage curves of the organic−inorganic hybrid thin films were measured using a Keithley 4200 semiconductor characterization system.

III. Results

A. Formation of Self-Assembled Organic Multilayers by Using MLD. Construction of self-assembled multilayers (SAMs) requires that the terminal groups of the monolayer be modified to a highly active one for the adsorption of the next monolayer. This is accomplished by means of a bifunctional surfactant possessing not only the usual polar head but also an apolar terminal function, which converts into a suitable polar group after completion of the adsorption step.[8,10] The present layer-by-layer synthesis of SAMs consists of three key steps, as shown in Figure 1a. First, an alkene-terminated alkylsiloxane self-assembled monolayer (SAM) was formed by exposing a substrate to 7-octenyltrichlorosilane (7-OTS) and water vapor in the ALD chamber. The $SiCl_3$ group of the 7-OTS molecule

(11) Kumagai, H.; Toyoda, K.; Kabayashi, K.; Obara, M.; Iimura, Y. *Appl. Phys. Lett.* **1997**, *70*, 2338.
(12) Ritala, M. *Appl. Surf. Sci.* **1997**, *112*, 223.
(13) Leskela, M.; Ritala, M. *J. Phys. IV* **1999**, *9*, 937.
(14) Jensen, J. M.; Oelkers, A. B.; Toivola, R.; Johnson, D. C.; Elam, J. W.; George, S. M. *Chem. Mater.* **2002**, *14*, 2276.
(15) Suntola, T. *Mater. Sci. Rep.* **1989**, *4*, 261.
(16) Leskela, M.; Ritala, M. *Thin Solid Films* **2002**, *409*, 138.
(17) Cameron, M. A.; Gartland, I. P.; Smith, J. A.; Diaz, S. F.; George, S. M. *Langmuir* **2000**, *16*, 7435.
(18) Lee, J. P.; Sung, M. M. *J. Am. Chem. Soc.* **2004**, *126*, 28.
(19) Shin, H.; Jeong, D-K.; Lee, J.; Sung, M. M.; Kim, J. *Adv. Mater.* **2004**, *16*, 1197.
(20) Seo, E. K.; Lee, J. W.; Sung-Suh, H. M.; Sung, M. M. *Chem. Mater.* **2004**, *16*, 1878.
(21) Park, M. H.; Jang, Y. J.; Sung-Suh, H. M.; Sung, M. M. *Langmuir* **2004**, *20*, 2257.
(22) Yoshimura, T.; Tatsuura, S.; Sotoyama, W. *Appl. Phys. Lett.* **1991**, *59*, 482.
(23) Du, Y.; George, S. M. *J. Phys. Chem. C* **2007**, *111*, 8509.
(24) Ishizaka, A.; Shiraki, Y. *J. Electrochem. Soc.* **1986**, *133*, 666.
(25) Rahyu, A.; Ritala, M. *Chem. Vap. Deposition* **2002**, *8*, 21.
(26) Dubowski, Y.; Vieceli, J.; Tobias, D. J.; Gomez, A. L.; Nizkorodov, S. A.; McIntire, T. M.; Finlayson-Pitts, B. J. *J. Phys. Chem. A* **2004**, *108*, 10473.
(27) Fiegland, L. R.; Fleur, M. M. S.; Morris, J. R. *Langmuir* **2005**, *21*, 2660.

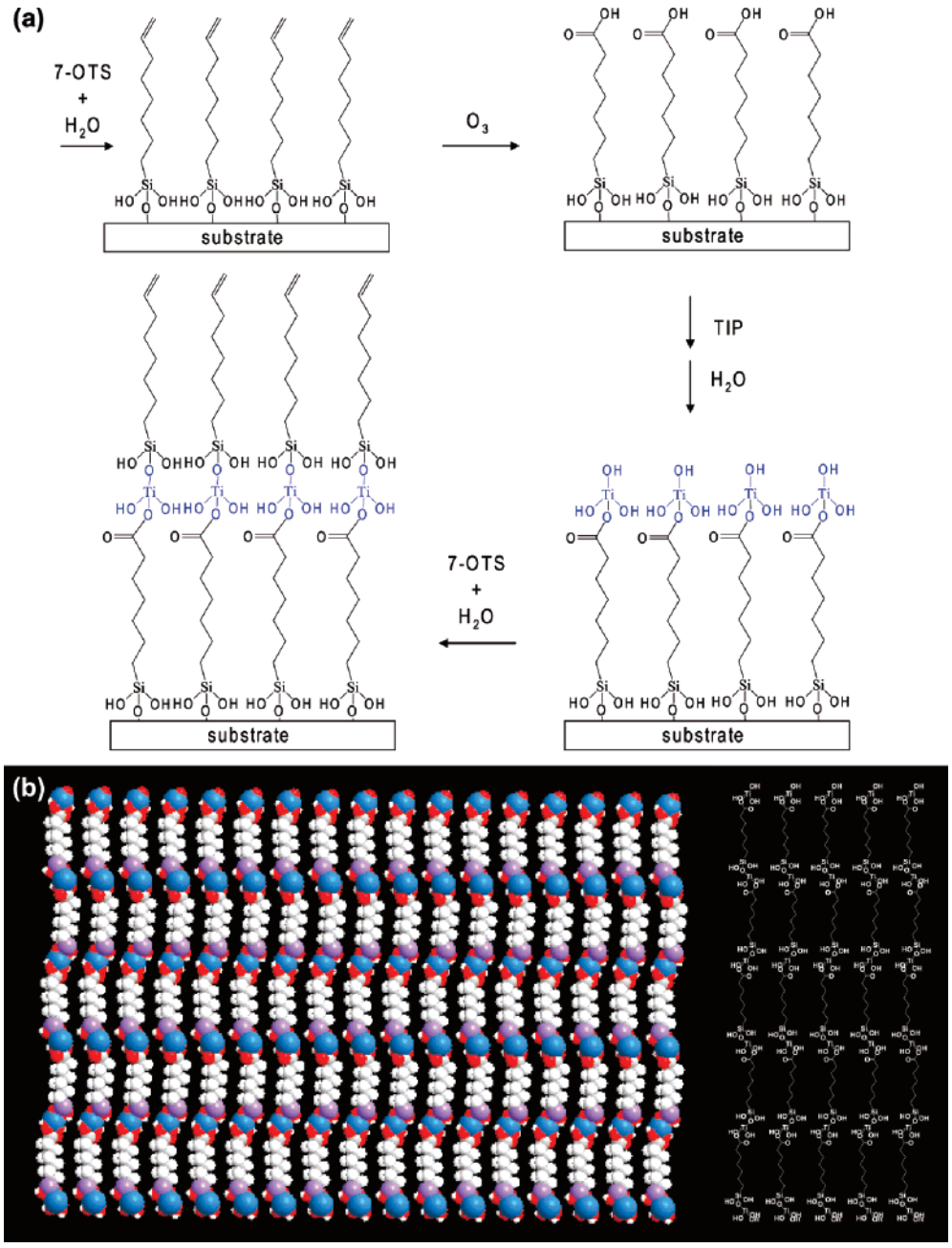

Figure 1. Self-assembled organic multilayers. (a) Schematic outline of the procedure to fabricate self-assembled organic multilayers by using molecular layer deposition. (b) Model structure of the self-assembled organic multilayers made by MLD.

was hydroxylated with an exchange reaction of water and enabled covalent attachment of the molecule to substrate surfaces rich in hydroxyl groups.

Second, the terminal vinyl group of the SAM was converted to a carboxylic group with ozone treatment. It has been found that the terminal C═C group of the SAM reacts with ozone to form a carboxylic acid.[26,27] In this experiment, the formation of the carboxylic group from the reaction of C═C-terminated SAM with gas-phase ozone was confirmed by X-ray photoelectron spectroscopy (XPS) analysis. Third, a highly active titanium hydroxyl was connected to the carboxylic acid-terminated SAM by using titanium isopropoxide adsorption followed by the exchange reaction of water. The titanium hydroxyl group of the SAM provides a highly active adsorption site for the anchoring of the next monolayer.

The alkylsiloxane self-assembled multilayers (SAMs) were grown under vacuum by repeated sequential adsorptions of C═C-terminated alkylsilane and titanium hydroxide with ozone activation, which was called "molecular layer deposition".[22,23] A model structure of the alkylsiloxane SAMs, made by the present MLD method, is shown in Figure 1b. In the case of an ideal multilayer structure, all trans alkyl chains with a chain axis are perpendicular to the substrate surface, and a silicon hydroxyl of the SAM is covalently bonded to a titanium hydroxyl, connected to a carboxylic acid of the SAM. For the ideal multilayer structure with completely perpendicular, fully extended alkyl chains, the expected monolayer thickness of the 7-OTS-based SAMs is about 12 Å.

The growing process of the SAMs, described in Figure 1a, was followed by wettability and XPS measurements. The water

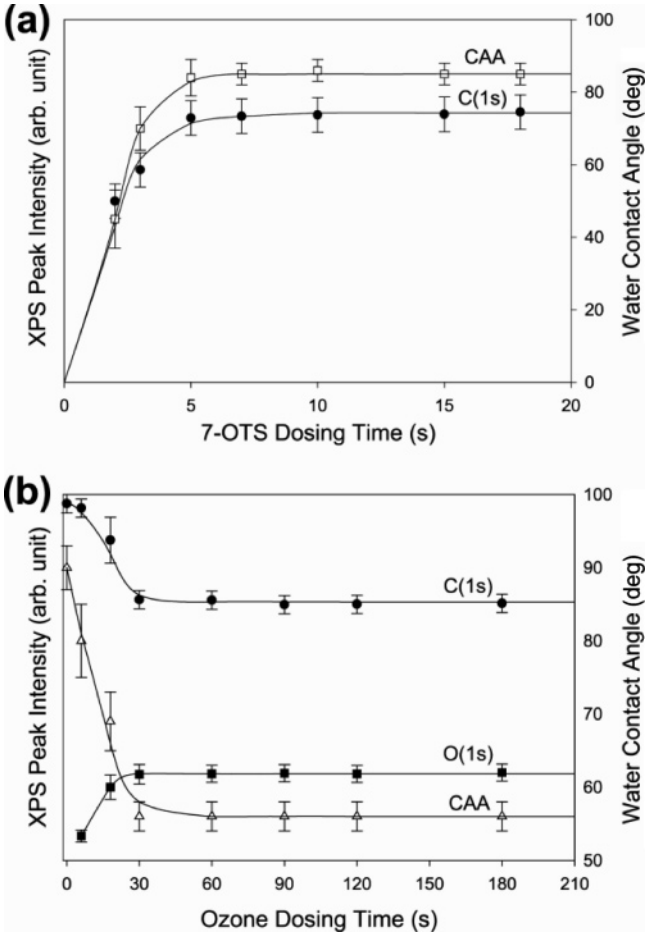

Figure 2. XP peak intensities and water contact angle of self-assembled monolayer: (a) water contact angles and C(1s) peak intensity as a function of 7-OTS dosing time; (b) water contact angles, C(1s), and O(1s) peak intensities as a function of ozone dosing time.

contact angles for the C═C and titanium hydroxyl-terminated SAM were 92° and 25°, respectively. The expected periodicities in the water contact angles and the XP peak intensities of the MLD steps alternating between a hydroxyl-rich (polar) and vinyl-rich (nonpolar) outer surface were observed. To verify that the formation of the C═C terminated SAM is really self-limiting, the pulse time of the 7-OTS molecule was varied between 1 and 20 s at 150−200 °C. Figure 2a shows that the water contact angles and C(1s) peak intensities as a function of the 7-OTS dosing time are saturated when the pulse time exceeds 5 s, which indicates that the growth is self-limiting.[28] The self-limiting character of the ozone reactions with the C═C terminated SAM was examined by measuring the water contact angles and XP peak intensities as a function of the ozone dosing time. The water contact angles and C(1s) peak intensities decrease by increasing the ozone dosing time up to 30 s and become saturated when the pulse time exceeds 30 s, as shown in Figure 2b. The O(1s) peak intensities also reach the highest value at the ozone dosing time of 30 s. These results suggest that the molecular layer deposition of the SAMs is self-limiting at temperatures of 150−200 °C.[28]

The thickness of the self-assembled multilayers versus the number of MLD cycles was measured using cross-sectional transmission electron microscopy, as shown in Figure 3a. These TEM images confirm the expectations for the monolayer thickness in the self-assembled multilayers and the MLD growth rate. The measured thickness of the monolayer was about 11 Å, which indicates that the chain is only tilted 25−30° from the surface normal. Figure 3b shows that the growth of the SAMs thickness is extremely linear relative to the number of cycles, indicating that the MLD conditions were sufficient for complete reaction.[28] The measured growth rate was about 11 Å per cycle. The AFM images of the multilayer stacks indicated very smooth and uniform surfaces, and the root-mean-square (rms) roughnesses of the surfaces were as low as 3.0 Å. In comparison, the surface roughness of the initial cleaned Si substrate is about 2.1 Å. Regardless of the cycle number, the surfaces of the self-assembled multilayers are as smooth as that of the initial cleaned Si substrate, indicating that the MLD growth occurs in a two-dimensional fashion via layer-by-layer growth. These results suggest that the molecular layer deposition of the self-assembled multilayer is self-limiting and proceeds via layer-by-layer growth, and that the MLD conditions are sufficient for complete reaction at temperatures of 150−200 °C. The thermal stability of the SAMs was studied using TEM, XPS, and contact angle analysis. The SAMs were stable in air up to temperatures of about 450 °C. Above 500 °C the SAMs slowly decomposed with the degradation of hydrocarbon fragments in the multilayers. TiO_2 polycrystals were observed on the surface following the decomposition of the SAMs at about 600 °C. This, together with the ability of the SAMs to survive the TEM preparation process, confirms that the monolayers are covalently bonded to each other.

B. Electrical Properties of Self-Assembled Organic Multilayers. To investigate the electrical properties of the self-assembled organic multilayers, the SAMs films were sandwiched between Pt metal electrodes by using MLD. A 100 nm thick Pt film was deposited on the Si (100) substrate by radio frequency magnetron sputtering. The SAMs films were grown on the bottom Pt electrodes by using MLD. The patterned top Pt electrodes (100 nm) were deposited onto the SAMs films using a shadow mask, and the gate area was about 1×10^{-4} cm^2. Figure 4a shows the leakage current density versus voltage characteristics of the Pt/SAMs/Pt capacitors. We measured the dependence of the leakage current density on the applied potential for a set of self-assembled multilayers with the thickness being systematically reduced from 99 to 1.1 nm. The positive bias means that the top metal electrode is positive with respect to the bottom metal electrode on Si. In general, the plot shows a decrease in current density with increasing film thickness. Direct tunneling is observed for film thicknesses less than 6.6 nm, while the other SAMs films with more than 6.6 nm do hardly show such direct tunneling.[29] With the thickness of 99 nm, our sample shows good gate leakage resistance. Figure 4b illustrates the frequency dependency of the dielectric constant of the SAMs at room temperature. The dielectric constant at 1 MHz for the samples is about 17, which remained almost constant in the frequency range from 100 Hz to 1 MHz for all the samples. The low electrical leakage and high dielectric constant suggests that the SAMs film is a good candidate for a high quality gate insulating film on flexible substrates.[29−33]

(28) Klaus, J. W.; Sneh, O.; George, S. M. *Science* **1997**, *278*, 1934.
(29) Lin, H. C.; Ye, P. D.; Wilk, G. D. *Appl. Phys. Lett.* **2005**, *87*, 182904.
(30) Vuillaume, D.; Boulas, C.; Collet, J.; Davidovits, J. V.; Rondelez, F. *Appl. Phys. Lett.* **1996**, *69*, 1646.

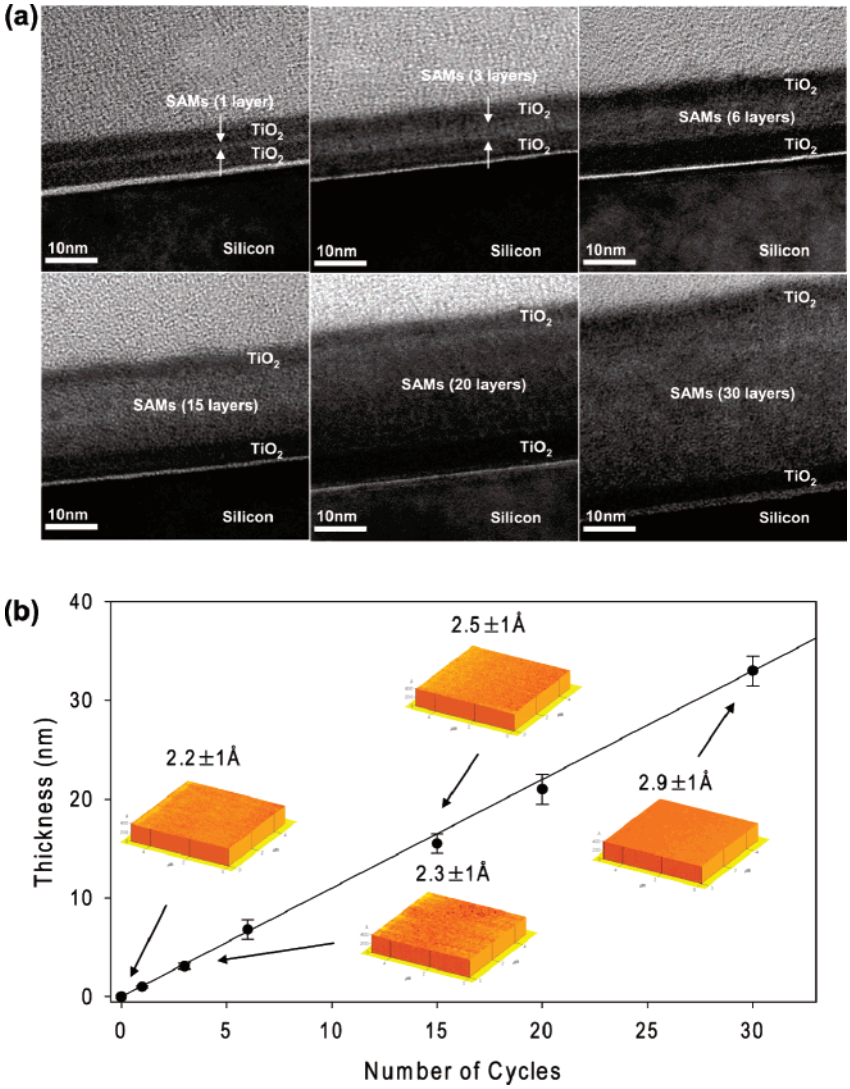

Figure 3. Self-assembled organic multilayers versus the number of MLD cycles: (a) TEM images of the self-assembled organic multilayers; (b) thickness and the root-mean-square (rms) roughness of the self-assembled organic multilayers.

To further demonstrate the electrical properties of the self-assembled organic multilayers, we have fabricated an organic pentacene thin-film transistor (TFT) adopting a 100 nm-thick SAMs film that was deposited on n^+-Si substrate. For good crystalline pentacene channel formation, the dielectric surface was terminated with a hydrophobic SAM. Pentacene (Aldrich Chem. Co., 99% purity) channels were patterned on the SAMs layer through a shadow mask at a substrate temperature at room temperature by thermal evaporation. We fixed the deposition rate to 1 Å/ s using an effusion cell (ALPHAPLUS Co., LTE-500S) in a vacuum chamber (base pressure $\sim 1 \times 10^{-7}$ Torr). The thickness of the pentacene film was 50 nm as monitored by a quartz crystal oscillator and confirmed by ellipsometry. Nominal channel length of the pentacene-TFT was 90 μm while channel width was 500 μm. Au was adopted as top-contact source/drain electrode. As shown in Figure 4c, typical drain current−drain voltage ($I_D - V_D$) output curves for a TFT was obtained from the pentacene−TFT with the SAMs dielectric, and the operating voltage was only −1 V for both gating and hole-transport. Maximum I_D level was around −0.24 μA under −1 V gate bias. According to the transfer characteristics ($I_D - V_G$) of Figure 4d, a high field effect mobility of 1.3 cm^2/V s was achieved in the saturation regime of $V_D = -1$ V along with an on/off current ratio of more than 500 and also with a threshold voltage of −0.48 V. Gate leakage current (I_G) was less than few nA. Our device mobility is quite comparable to or even surpassing previous results from low-voltage-driven organic TFTs with various dielectrics,[34−39] while our operating voltage, 1 V is the lowest among those of other TFTs. Since the SAMs dielectric has a high dielectric constant (~17) and a

(31) Collet, J.; Tharaud, O.; Chapoton, A.; Vuillaume, D. *Appl. Phys. Lett.* **2000**, *76*, 1941.
(32) Kobayashi, S.; Nishikawa, T.; Takenobu, T.; Mori, S.; Shimoda, T.; Mitani, T.; Shimotani, H.; Yoshimoto, N.; Ogawa, S.; Iwasa, Y. *Nat. Mater.* **2004**, *3*, 317.
(33) Muccini, M. *Nat. Mater.* **2006**, *5*, 605.
(34) Panzer, M. J.; Newman, C. R.; Frisbie, C. D. *Appl. Phys. Lett*, **2005**, *86*, 103503.
(35) Dimitrakopoulos, C. D.; Purushothaman, S.; Kymissis, J.; Callegari, A.; Shaw, J. M. *Science*, **1999**, *283*, 822.
(36) Halik, M.; Klauk, H.; Zschieschang, U.; Schmid, G.; Dehm, C.; Schutz, M.; Malsch, S.; Effenberger, F.; Brunnbauer, M.; Stellacci, F. *Nature*, **2004**, *431*, 963.
(37) Liang, Y.; Dong, G.; Hu, Y.; Wang, L.; Qiu, Y. *Appl. Phys. Lett*, **2005**, *86*, 132101.
(38) Kim, K. D.; Song, C. K. *Appl. Phys. Lett*, **2006**, *88*, 233508.
(39) Hwang, D. K.; Kim, C. S.; Choi, J. M.; Lee, K.; Park, J. H.; Kim, E.; Baik, H. K.; Kim, J. H.; Im, S. *Adv. Mater*, **2006**, *18*, 2299.

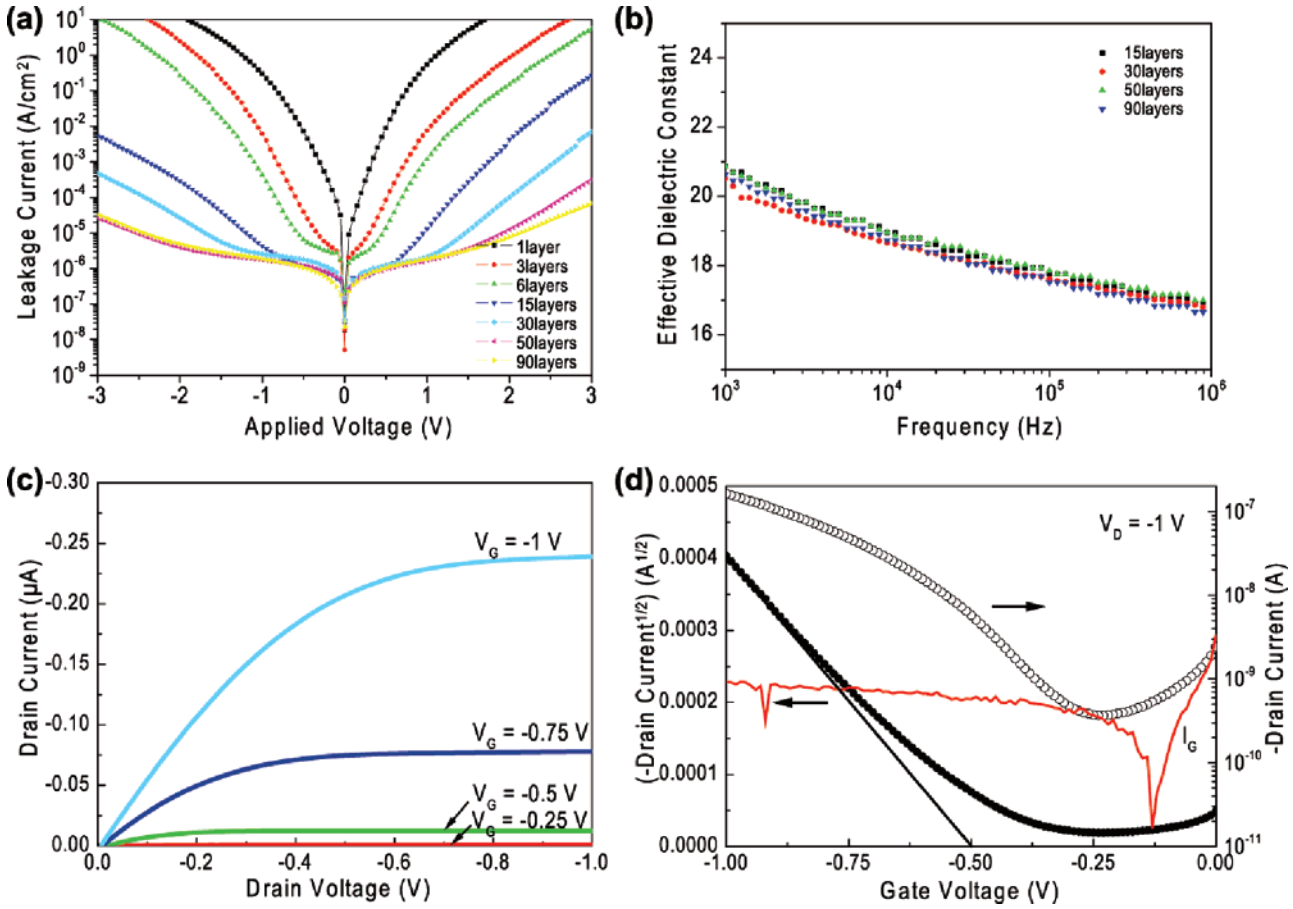

Figure 4. Electrical properties of the self-assembled organic multilayers: (a) leakage current density as a function of applied voltage; (b) effective dielectric constant as a function of frequency; (c) drain current-drain voltage ($I_D - V_D$) output curves for a TFT; (d) drain current−gate voltage ($I_D - V_G$) transfer curves and gate current−gate voltage ($I_G - V_G$) curves for the gate leakage levels for a TFT.

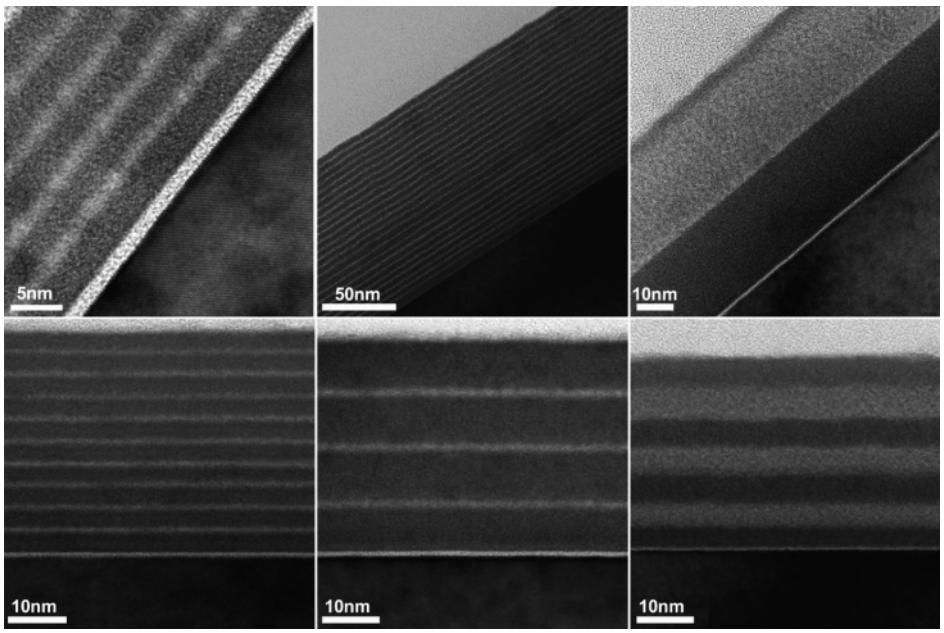

Figure 5. TEM images of self-assembled organic multilayer/TiO_2 nanolaminate films made by using MLD with ALD (white is the SAMs layer, and black is the TiO_2 layer).

decent dielectric strength as well, it is regarded that a low-voltage operation of pentacene-TFT is very possible without serious gate leakage.

C. Formation of SAMs/TiO_2 Nanolaminate Films by Using MLD−ALD. The SAMs/TiO_2 nanolaminate films were grown by using MLD, combined with ALD, in the same deposition chamber. Several self-assembled organic-TiO_2 inorganic nanolaminate films were deposited on Si (100) substrates at 150−200 °C, as shown in Figure 5a. The Si substrates were first coated with 2 nm of TiO_2 and the top layer of each nanolaminate

film was TiO_2. The thicknesses of SAMs and TiO_2 nanolayers in each sample were controlled by adjusting the number of MLD and ALD cycles with SAMs and TiO_2 growth rates of about 11 and 0.6 Å/cycle, respectively. The TEM images provide direct observation of the superlattice structures and confirm the expectations for the individual SAMs and TiO_2 nanolayers in the nanolaminate films. The layers appear to be relatively uniform, which is confirmed by AFM. From energy dispersive X-ray spectroscopy (EDS) analysis, the concentration of C atom was about 40.8% at the SAMs layer, whereas only Ti and O atoms were detected at the TiO_2 layer.

D. Electrical Properties of SAMs/TiO_2 Nanolaminate Films. Two-terminal electrical bistable devices were fabricated using the present organic−inorganic hybrid films sandwiched between Al metal wires to form an 8 × 8 crossbar. The patterned Al electrodes were vapor-deposited on the Si substrates with a thermally grown oxide. The SAMs/TiO_2 nanolaminate films were grown on the entire substrate, including the bottom Al electrodes. All nanolaminated films studied were approximately 14.4 nm thick and consist of four [SAMs (1.1 nm)/TiO_2 (2 nm)] bilayer subunits. The top Al electrodes (100 nm) were deposited on the organic−inorganic films, perpendicular to the bottom electrodes. The lines of the top and bottom electrodes were about 100 μm wide and were separated by about 100 μm.

A typical current−voltage ($I-V$) characteristic of the organic−inorganic hybrid thin films, recorded in the voltage control mode, is shown in Figure 6a. As-prepared samples show asymmetric $I-V$ characteristics within a bias range from −2.8 to 2.8 V (black line). When we swept the bias of the bottom electrode with respect to the top electrode from zero to negative values, the current suddenly increased at about −2.8 V to a limit value imposed by the current compliance and the films switched into a low resistance state (red line). Subsequently sweeping the voltage to positive values above 2.8 V led to a sudden decrease of the current and changed the films into a high resistance state. Hence switching behavior leads to a pronounced hysteretic $I-V$ characteristic with two bistable resistance states. The cutoff at large current in Figure 6a is due to imposed compliance on the current source to avoid sample damage. The apparent asymmetry of the $I-V$ characteristic from the symmetric memory device (Al/TiO_2/SAM/TiO_2/Al) may be attributed to the asymmetric interfacial structures between the top and bottom Al/TiO_2 interfaces. Although there was a native aluminum oxide layer about 2 nm thick in the bottom Al/TiO_2 interface, the top interface consisted of the TiO_2 and metallic aluminum without a native aluminum oxide layer. Therefore, the memory device structure is asymmetric at the nanometer scale.

The switching operation of the bistable memory device in the pulse mode is illustrated in Figure 6b. The memory device can be switched into the low-resistance state (the ON state) with a negative voltage pulse of 10 ms. After applying a positive pulse of 10ms, the "information" written to the device is erased and the high-resistance state (the OFF state) is recovered. Between each writing and erasing pulses, the resistance of the state was read for 4 s at −1 V. This switching behavior can be repeated reproducibly more than 10^6 times. We also have performed a retention test of the memory device and found little change over 1 year. The decrease of the readout current of the low resistance state after 1 year was found to be less 10%.

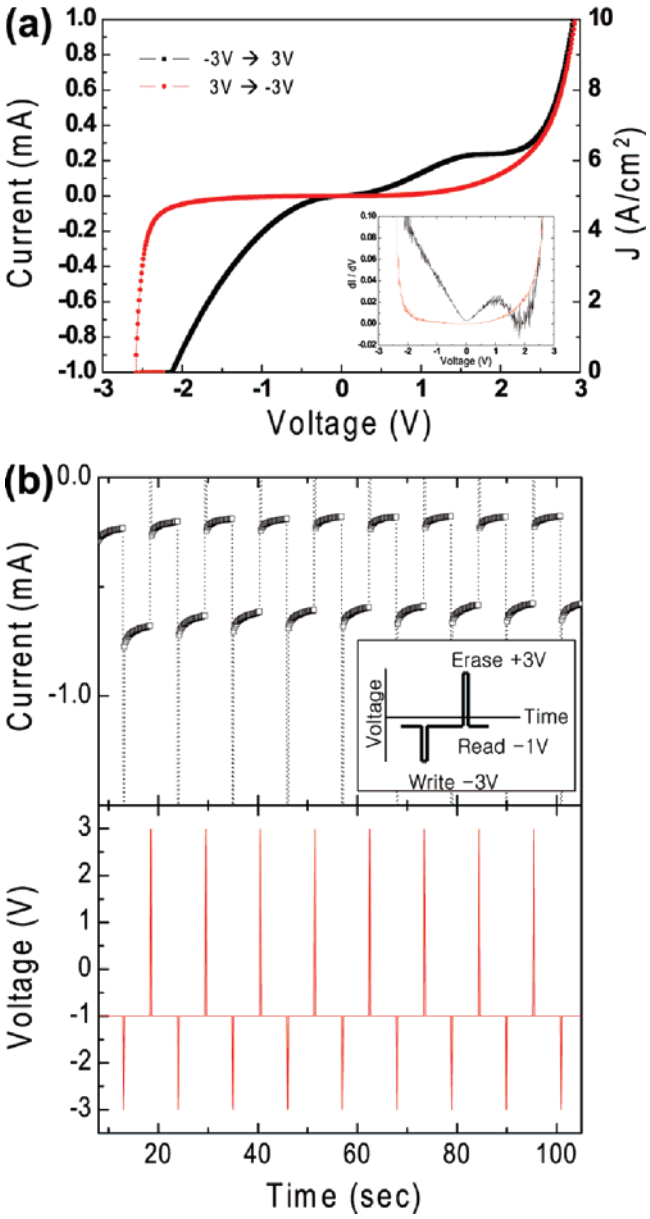

Figure 6. (a) Current−voltage curves for the SAMs/TiO_2 nanolaminate films measured from −2.8 to +2.8 V and the differential conductance vs voltage plot was shown as the inset. (b) Switching performance of the SAMs/TiO_2 nanolaminate films in the pulse mode (the lower graph shows applied voltage vs time and the upper graph displays the corresponding current change vs time) and the WRITE−READ−ERASE−READ pulse cycle was shown as the inset.

A detailed analysis of the conduction behaviors showed that the hysteretic switching of the nanolaminated films resulted from the charge trapping and detrapping of the defects in the TiO_2 layer or the interfacial layers,[40] but the nature of the defects deserves further study. Because of the very thin film thickness (∼14.4 nm) and very high electric field, the defects can move relatively freely in the thin films so that the distribution of defects becomes homogeneous after a long time. The organic SAM layers function as diffusion barriers for the defects. In the device with the single TiO_2 layer (∼14 nm) without the organic SAMs layer, the memory effect disappeared after a few days. The simple structure of the devices, a large endurance and a long retention time demonstrate the potential application

(40) Argall, F. *Solid-State Electron.* **1968**, *11*, 535.

of the organic−inorganic hybrid films as nonvolatile memory materials. The resistance at each cross point of the crossbar can be switched reversibly. By using each cross point as an active memory cell, crossbar circuits were operated as rewritable and nonvolatile memory,[41−45] even on the flexible substrates.

IV. Conclusions

We developed a new layer-by-layer growth method of self-assembled organic multilayers based on gas-phase reactions. The molecular layer deposition method is self-limiting with layer-by-layer growth, and perfectly compatible with the atomic layer deposition (ALD) method. The SAMs films prepared exhibit good thermal and mechanical stability and various unique electrical properties. The MLD method with ALD was applied to the preparation of self-assembled organic−inorganic hybrid nanolaminate films in the ALD chamber. Two-terminal electrical bistable devices were fabricated using the present organic−inorganic hybrid films sandwiched between Al metal wires to form an 8 × 8 crossbar. The advantages of the MLD method with ALD include accurate control of film thickness, large-scale uniformity, highly conformal layering, and sharp interfaces. The MLD method with ALD is an ideal fabrication technique for various organic−inorganic hybrid superlattices and, furthermore, can be applied to fabricate organic−inorganic−metal hybrid superlattices.

Acknowledgment. This work was supported by the Korea Science and Engineering Foundation (KOSEF) grant funded by the Korea government (MOST) (No. R01-2007-000-10402-0) and by the KICOS through a grant provided by MOST (No. K20501000002-07-E0100-00210). This work was also partially supported by Seoul R&BD Program (10919) .

JA075664O

(41) Beck, A.; Bednorz, J. G.; Gerber, C.; Rossel, C.; Widmer, D. *Appl. Phys. Lett.* **2000**, *77*, 139.
(42) Ma, L.; Pyo, S.; Quyang, J.; Xu, Q.; Yang, Y. *Appl. Phys. Lett.* **2003**, *82*, 1419.
(43) Lai, Y.; Tu, C.; Kwong, D.; Chen, J. S. *Appl. Phys. Lett.* **2005**, *87*, 87.
(44) Rozenberg, M. J.; Inoue, I. H.; Sanchez, M. J. *Phys. Rev. Lett.* **2004**, *92*, 178302.
(45) Akkerman, H. B.; Blom, P. W. M.; de Leeuw, D. M.; de Boer, B. *Nature* **2006**, *441*, 69.